20th Australasian Fluid Mechanics Conference
Perth, Australia
5-8 December 2016

Modelling the spreading of a liquid droplet on a super-hydrophobic surface using the Multiphase Lattice Boltzmann method

H. Rashidian and M. Sellier

Department of Mechanical Engineering
University of Canterbury, Christchurch 8041, New Zealand

Abstract

Nowadays, the development of artificial super-hydrophobic surfaces has led to several technological advances such as self-cleaning surfaces, anti-icing surfaces, anti-fouling surfaces and reduced-drag surfaces. A key feature of many synthetic super-hydrophobic surfaces is the topographical pattern imprinted on them in the form of arrays of micron-sized pillars. In this study, a two-dimensional Multiphase Lattice Boltzmann code is developed for modelling the spreading of a droplet on a surface with two ridges. This paper reports an effect of the geometric parameters of the textured surfaces on different outcomes of the wetting front during the spreading of the droplet.

Introduction

Super-hydrophobic behaviour has been observed in leaves of plants, wings of butterfly, beetle exoskeleton and other natural objects [1,5]. The lotus leaf is the best known example of super-hydrophobic surface in nature [6] and has inspired the fabrication of artificial super-hydrophobic surfaces [7]. Super-hydrophobicity has been an important area of research over decades and the interaction between liquid and textured surfaces has attracted much attention in scientific communities and industries [8,12]. Recently, researchers have performed many experiments using high speed photography techniques about several important fields such as drop impact on super-hydrophobic surfaces, spreading dynamics and drop splashing on a textured surface [13,17]. The authors of these studies have investigated the effects of micro-pillars, the fluid's inertia, the surface tension and the air pressure on a droplet which impacts on a textured surface. In parallel, many numerical simulations and CFD approaches have been proposed to model the wetting on smooth and rough surfaces, equilibrium and transition states, moving contact line problems [17,21].

When a water droplet sits on a surface, a contact angle exists at the droplet edge where the liquid-gas interface meets the solid substrate. For an ideal solid surface, the equilibrium contact angle (θ_E) is defined by the Young's Equation [22]:

$$COS\theta_E = \frac{\gamma_{SO} - \gamma_{SL}}{\gamma} \tag{1}$$

where γ_{SO} , γ_{SL} and γ denote the interfacial tension between solid-gas, solid-liquid and liquid-gas respectively. A contact angle less than 90° indicates is high wettability (hydrophilicity) and a contact angle greater than 90° correspond to low wettability (hydrophobicity). Therefore the behavior of the contact line is a crucial parameter in wetting phenomena. A super-hydrophobic surface has a contact angle greater than 150°.

The characteristics of super-hydrophobic surfaces are two-fold: they are low energy surfaces which means water repellent and covered by a hierarchy of micro-structures. For surfaces with microstructures, it is well known that two wetting states may exist: the Wenzel state where the liquid completely fills the space between the pillars and the Cassie-Baxter state where the droplet effectively sits on the top of the micro-pillars with an air pocket underneath. In fact, the Cassie-Baxter state leads to a very low contract angle hysteresis and therefore a very slippery surface on which droplets are highly mobile while the Wenzel state leads to a stickier surface where droplets are much harder to displace.

The apparent contact angle of a droplet in the Wenzel state is given by [23]:

$$COS\theta_W = rCOS\theta_W \tag{2}$$

where r denotes the roughness factor defined the ratio of the actual surface area to the planar area.

For the Cassie-Baxter state, the apparent contact angle is determined as [24]:

$$COS\theta_{CB} = (-1 + \Phi(1 + COS\theta_E) \tag{3}$$

where Φ denotes the ratio of the pillars top surface area to the substrate total base area.

Droplet impact conditions are characterized by the dimensionless Reynolds and Weber Numbers which balance the inertia force with the viscous force and the capillary force, respectively:

$$Re = \frac{2\rho V r}{\mu} \tag{4}$$

$$We = \frac{2\rho V^2 r}{\sigma} \tag{5}$$

where ρ, μ and σ are the density, viscosity and surface tension of the liquid, respectively. D denotes the diameter of the droplet and V refers to the impact velocity.

This paper aims to introduce a two dimensional multiphase lattice Boltzmann code for simulation the impact and spreading of a droplet on a super-hydrophobic surface with two ridges. Also, the influence of the geometrical parameters on different outcomes of the contact line during the spreading is investigated.

The remainder of the paper is arranged as follows. The next section introduces the multiphase lattice Boltzmann method which is applied in this study. A validation case is presented in the third section to show the ability of the lattice Boltzmann method for modelling the wetting phenomena. Modelling results are presented in the section 4 and then the effects of the topography on the final state of the wetting are discussed. Finally, section 5 concludes the paper.

Methodology

The Lattice Boltzmann Method (LBM) has emerged as a mesoscopic approach for modelling multi-phase flows and interfacial dynamics problems. The principal idea behind the

LBM is to solve a discrete Boltzmann equation for particle distribution functions $f(\boldsymbol{x},t)$ through a simple algorithm consisting of a streaming term which models the particle distribution advection along the lattice link and a collision process which models the rate of change in the particle distribution. The discretised Boltzmann equation can be written as [25]:

$$f_k(\boldsymbol{x}+\boldsymbol{e_k},t+1)=f_k(\boldsymbol{x},t)+\frac{1}{\tau}\left[f_k^{eq}(\boldsymbol{x},t)-f_k(\boldsymbol{x},t)\right] \quad (6)$$

Equation (6) is based on the Bhatnagar-Gross-Krook (BGK) approximation. $\boldsymbol{e_k}$ is the microscopic velocity. In this work, we choose the D2Q9 model which has nine velocity vectors such that k = 0,…,8. τ represents the relaxation time which is related to the kinematic viscosity by υ = (τ -0.5) / 3. Moreover, f^{eq} denotes the equilibrium distribution function and for the D2Q9 model is defined as:

$$f_k^{eq}(\boldsymbol{x},t)=\omega_k\rho\left[1+3(\boldsymbol{e_k}.\boldsymbol{u})+\frac{9}{2}(\boldsymbol{e_k}.\boldsymbol{u})^2-\frac{3}{2}\boldsymbol{u}^2\right] \quad (7)$$

where $\boldsymbol{u}$ is the macroscopic velocity. ω denotes the weight factor which is 4/9 for k=0, 1/9 for k=1,2,3,4 is and 1/36 for k=5,6,7,8. The macroscopic moments can be obtained as:

$$\rho=\sum_k f_k \quad (8)$$

$$\rho\boldsymbol{u}=\sum_k f_k\boldsymbol{e_k} \quad (9)$$

The no-slip boundary condition which is called the bounceback boundaries in LBM is applied at the solid-liquid interface because it is particularly simple and efficient. Periodic boundary condition is used for the other boundaries.

To consider the interaction between fluid-fluid and solid-fluid, the single-component multiphase (SCMP) Shan-Chen (SC) model [26] is implemented. In the SCMP model, incorporating the forcing item into the correlated lattice Boltzmann equation changes the equation of state (EOS) from an ideal gas to a non - ideal and non-monotonic one. The inter particle force is given by [27]:

$$F(\boldsymbol{x},t)=-G\psi(\boldsymbol{x},t)\sum_K\omega_K\psi(\boldsymbol{x}+\boldsymbol{e_k}\Delta t,t)\boldsymbol{e_k} \quad (10)$$

where G is a strength control parameter of the force and ψ denotes an interaction potential. Moreover, the Carnahan and Starling (C-S) EOS is applied that is obtained as:

$$P=\rho RT\frac{1+b\rho/4+(b\rho/4)^2-(b\rho/4)^3}{(1-b\rho/4)^3}-a\rho^2 \quad (11)$$

with following Yuan and Schafer: a=1, b=4 and R=1 [28]. Also during simulations, the relaxation time, gas density and liquid density are 1, 0.0285 and 0.285, respectively. The effect of gravity is ignored in this study.

Validation

The modelling of the static contact angle on the smooth surface is carried out as a validation case. Various contact angles can be obtained through setting a parameter which is a value between the densities of liquid phase and gas phase. The size of computational domain is 300 lu by 60 lu and the diameter of the droplet is adjusted 40 lu. At the beginning of the simulation, a liquid droplet is in contact with the surface. After reaching an equilibrium state, the static contact angle is measured. The simulation of the droplet with different angels 165°, 135°, 90°and 60° are obtained and demonstrated in figure 1. There is a good similarity between the computational models and the theoretical values [29].

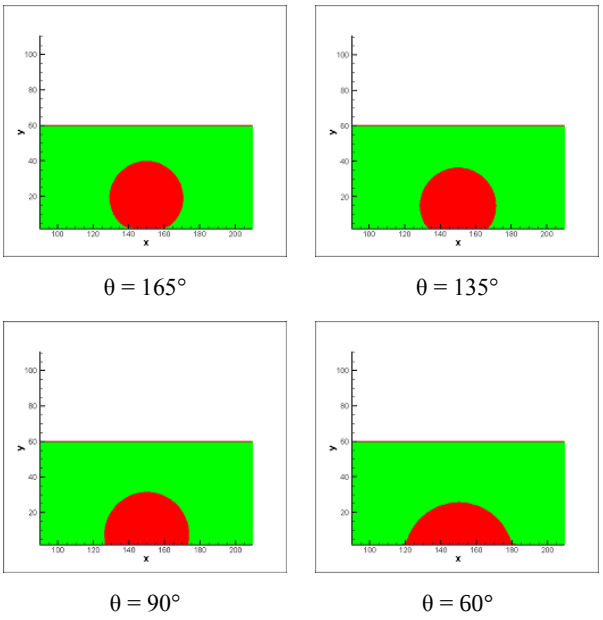

Figure 1. Modelling of the static contact angle on the smooth surface

Numerical results and discussion

To investigate the behaviour of the droplet spreading on the surface with two ridges, the substrate is arranged as shown in Figure 2. A droplet with radius r =50 lu and initial velocity V=0.1 lu/ts impacts at the middle of the spacing (S) between two posts. Both ridges have a same shape and the equilibrium contact angle is set up at 135° for all points of the surface. In this part of study, the aspect ratio (W/h) is unity where w and h denote the width and height of posts, respectively. During simulations, the weber number and Reynolds number are constant. Four different cases which make with various widths and spaces of ridges are given by table 1:

case	h (lu)	W (lu)	S (lu)
I	10	10	10
2	10	10	20
3	20	20	10
4	20	20	20

Table 1. Four different simulation cases

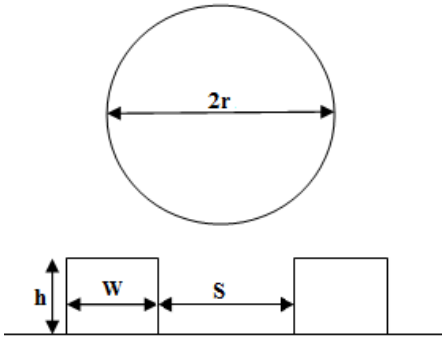

Figure 2. Geometry of simulations

Figure 3 shows simulation results at the final state attained for the four cases. In the first case, the droplet wets the top of both ridges

but an air bubble appears directly under the droplet in the spacing between two posts due to air trapped under the falling drop. It is observed that the Wenzel state occurs in the second case where the liquid completely fills the space between the two posts from the middle of the droplet (mushroom state). In cases 3 and 4, the droplet is suspended on the posts and the air pockets are entrapped below the droplet and it is exactly the definition of the Cassie-Baxter state. When comparing both cases, it can be seen that the only difference between them is the contact angle which is greater for case 4 than for case 3.

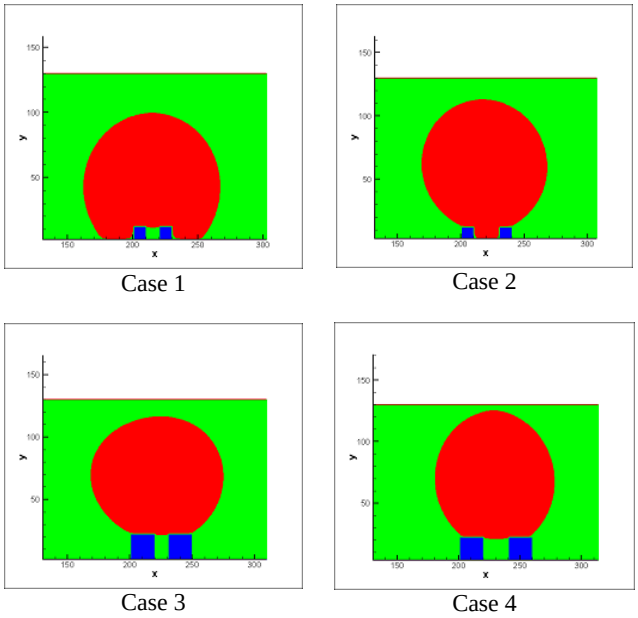

Case 1 Case 2

Case 3 Case 4

Figure 3. Modelling of the impact droplet on the two ridges surface

To get a better understanding of the effect of the textured surface on the outcomes, this simulation is extended for a wide range of geometric parameters. The aspect ratio is unity as previously. The width and space are chosen in the range between 5 lu to 20 lu with a step equal 5. The modelling results are collected in Table 2. It can be seen that the Cassie-Baxter model occurs as 2W+S is equal or greater than the radius of the droplet. In other cases and when 2W+S is less than the droplet radius, two main state are observed; first the air bubble exists as the spacing values are 5 and 10 and second the Wenzel model happens for the spacing S=15 and S=20.

h (lu)	W (lu)	S (lu)	Outcome
20	20	20	Cassie and Baxter
20	20	15	Cassie and Baxter
20	20	10	Cassie and Baxter
20	20	5	Engulfed (non-symmetric)
15	15	20	Cassie and Baxter
15	15	15	Wenzel (mushroom state)
15	15	10	Engulfed (non-symmetric)
15	15	5	Engulfed
10	10	20	Wenzel (mushroom state)
10	10	15	Wenzel (non-symmetric)
10	10	10	Engulfed
10	10	5	Engulfed
5	5	20	Wenzel (penetration)
5	5	15	Wenzel (penetration)
5	5	10	Engulfed
5	5	5	Engulfed

Table 3. Summary of droplet state outcomes for a wide range of geometrical parameters

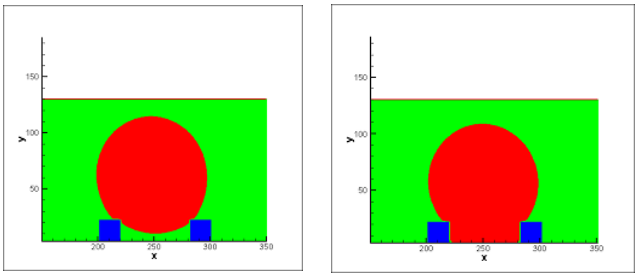

a b

Figure 4. Effect of the parameter S/2r on the wetting state for W = h =20 lu (a) The Cassie and Baxter state as S/2r = 0.61 and (b) The Wenzel state as S/2r = 0.62.

It should be mentioned that the spacing value over the size of droplet (S/2r) is another significant parameter which should be considered. If this parameter has a value which is greater than its threshold value it appears that the droplet is in the Wenzel state instead of the Cassie-Baxter state. For example, as shown in Figure 4, this threshold value is 0.62 when W = h =20. In other word, the state is Cassie and Baxter model from S/2r =0.08 until S/2r = 0.61(Figure 4a). But the state changes to the Wenzel model as this value sets on 0.62(Figure 4b).

Beside the width and spacing of the ridge, the effect of the ridge height is also important. In this section the aspect ratio is not unity and for making a good comparison, the width and spacing are equal. The simulation results are depicted in Figure 5. It can be seen that the state of the wetting is not significantly influenced by the height of ridge as 2W + S is less than the radius of droplet. In other word, when the width and space are chosen in the range between 5 lu to 15 lu, the outcome is not changed by increasing or decreasing the ridge height. But it is observed that for W=S=20 lu, the outcome depends on the height of posts. It means that the state is the Cassie-Baxter model as the ridge height has a value between 15 lu to 25 lu. If the height of posts is less than 15 lu then the mushroom Wenzel state takes place and whenever this value is equal or greater than 29 lu, the droplet penetrates both ridges but an air bubble exists in the spacing between two posts. It should be mentioned that a non-symmetric state occurs for h=26, 27 and 28 lu. In these cases either the droplet has not a symmetric condition (h=26) or the droplet does not sit on the posts completely (h=27 and 28).

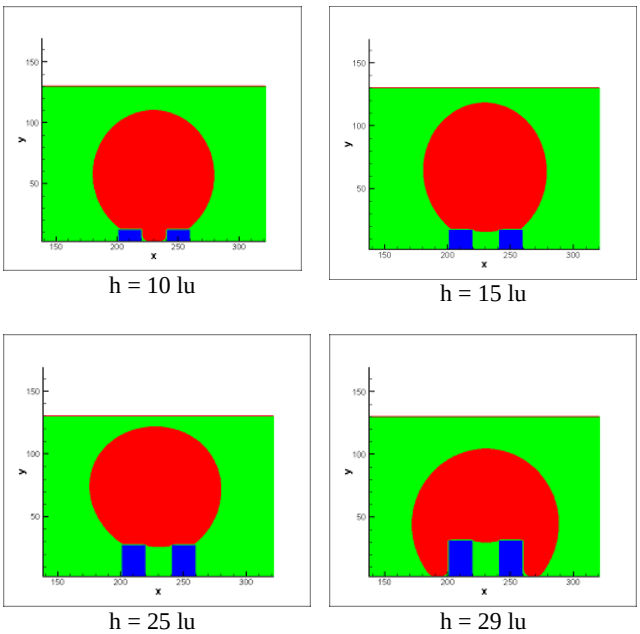

h = 10 lu h = 15 lu

h = 25 lu h = 29 lu

Figure 5. Simulation results of influence the ridge height on the wetting state when W=S=20 lu

Conclusions

This study has presented numerical results using the multiphase Lattice Boltzmann method based on the single-component multiphase Shan-Chen model to simulate the droplet impact on a two ridges textured super-hydrophobic surface. The results have shown that this method can be a powerful tool to investigate the wetting phenomenon. The influences of the geometric parameters such as 2W+S, S/2r and the ridge height on the behaviour of the droplet have been investigated. Simulation results have demonstrated that the Cassie-Baxter state occurs only as 2W+S becomes a sufficiently large value and also S/2r has an amount which is less than a threshold value. Finally the outcome is not significantly influenced by the post height for a small 2W + S value. Several questions remain open. For example, by incorporating various Weber numbers whether the outcomes of the contact line during the spreading will be changed.

References

[1] Guo Z, Liu W, Su BL. Superhydrophobic surfaces: from natural to biomimetic to functional. Journal of colloid and interface science. 2011 Jan 15;353(2):335-55.

[2] Feng L, Li S, Li Y, Li H, Zhang L, Zhai J, Song Y, Liu B, Jiang L, Zhu D. Super-hydrophobic surfaces: from natural to artificial. Advanced materials. 2002 Dec 17;14(24):1857-60.

[3] Feng XQ, Gao X, Wu Z, Jiang L, Zheng QS. Superior water repellency of water strider legs with hierarchical structures: experiments and analysis. Langmuir. 2007 Apr 24;23(9):4892-6.

[4] Zheng Y, Gao X, Jiang L. Directional adhesion of superhydrophobic butterfly wings. Soft Matter. 2007;3(2):178-82.

[5] Bormashenko E, Bormashenko Y, Stein T, Whyman G, Bormashenko E. Why do pigeon feathers repel water? Hydrophobicity of pennae, Cassie–Baxter wetting hypothesis and Cassie–Wenzel capillarity-induced wetting transition. Journal of colloid and interface science. 2007 Jul 1;311(1):212-6.

[6] Quéré D, Reyssat M. Non-adhesive lotus and other hydrophobic materials. Philosophical Transactions of the Royal Society of London A: Mathematical, Physical and Engineering Sciences. 2008 May 13;366(1870):1539-56.

[7] Celia E, Darmanin T, de Givenchy ET, Amigoni S, Guittard F. Recent advances in designing superhydrophobic surfaces. Journal of colloid and interface science. 2013 Jul 15;402:1-8.

[8] Zhai L, Berg MC, Cebeci FC, Kim Y, Milwid JM, Rubner MF, Cohen RE. Patterned superhydrophobic surfaces: toward a synthetic mimic of the Namib Desert beetle. Nano Letters. 2006 Jun 14;6(6):1213-7.

[9] Dorrer C, Ruehe J. Wetting of silicon nanograss: from superhydrophilic to superhydrophobic surfaces. Advanced Materials. 2008 Jan 7;20(1):159-63.

[10] Feng XJ, Jiang L. Design and creation of superwetting/antiwetting surfaces. Advanced Materials. 2006 Dec 4;18(23):3063-78.

[11] Guo Z, Zhou F, Hao J, Liu W. Stable biomimetic super-hydrophobic engineering materials. Journal of the American Chemical Society. 2005 Nov 16;127(45):15670-1.

[12] Jeong DW, Shin UH, Kim JH, Kim SH, Lee HW, Kim JM. Stable hierarchical superhydrophobic surfaces based on vertically aligned carbon nanotube forests modified with conformal silicone coating. Carbon. 2014 Nov 30;79:442-9.

[13] Fritsch A, Willmott GR, Taylor M. Superhydrophobic New Zealand leaves: contact angle and drop impact experiments. Journal of the Royal Society of New Zealand. 2013 Dec 1;43(4):198-210.

[14] Kim SJ, Kim J, Moon MW, Lee KR, Kim HY. Experimental study of drop spreading on textured superhydrophilic surfaces. Physics of Fluids (1994-present). 2013 Sep 1;25(9):092110.

[15] Van der Veen RC, Hendrix MH, Tran T, Sun C, Tsai PA, Lohse D. How microstructures affect air film dynamics prior to drop impact. Soft matter. 2014;10(21):3703-7.

[16] Tsai P, CA van der Veen R, van de Raa M, Lohse D. How micropatterns and air pressure affect splashing on surfaces. Langmuir. 2010 Sep 22;26(20):16090-5.

[17] Liu Y, Moevius L, Xu X, Qian T, Yeomans JM, Wang Z. Pancake bouncing on superhydrophobic surfaces. Nature Physics. 2014 Jul 1;10(7):515-9.

[18] Dupuis A, Yeomans JM. Modeling droplets on superhydrophobic surfaces: equilibrium states and transitions. Langmuir. 2005 Mar 15;21(6):2624-9.

[19] Osman M, Rasool R, Sauer RA. Computational aspects of self-cleaning surface mechanisms. Advances in Contact Angle, Wettability and Adhesion. 2013;1:109-30.

[20] Sellier M. Modelling the wetting of a solid occlusion by a liquid film. International Journal of Multiphase Flow. 2015 May 31;71:66-73.

[21] Ellis AS, Smith FT, White AH. Droplet impact on to a rough surface. The Quarterly Journal of Mechanics and Applied Mathematics. 2011 May 1;64(2):107-39.

[22] De Gennes PG, Brochard-Wyart F, Quéré D. Capillarity and wetting phenomena: drops, bubbles, pearls, waves. Springer Science & Business Media; 2013 Mar 20.

[23] Wenzel RN. Resistance of solid surfaces to wetting by water. Industrial & Engineering Chemistry. 1936 Aug;28(8):988-94.

[24] Cassie AB, Baxter S. Wettability of porous surfaces. Transactions of the Faraday Society. 1944;40:546-51.

[25] Mohamad AA. Lattice Boltzmann method: fundamentals and engineering applications with computer codes. Springer Science & Business Media; 2011 Jun 27.

[26] Shan X, Chen H. Simulation of nonideal gases and liquid-gas phase transitions by the lattice Boltzmann equation. Physical Review E. 1994 Apr 1;49(4):2941.

[27] Huang H, Sukop M, Lu X. Multiphase lattice Boltzmann methods: Theory and application. John Wiley & Sons; 2015 Jun 11.

[28] Yuan P, Schaefer L. Equations of state in a lattice Boltzmann model. Physics of Fluids (1994-present). 2006 Apr 1;18(4):042101.

[29] Benzi R, Biferale L, Sbragaglia M, Succi S, Toschi F. Mesoscopic modeling of a two-phase flow in the presence of boundaries: the contact angle. Physical Review E. 2006 Aug 30;74(2):021509.